

Supplement of Atmos. Chem. Phys., 20, 2017–2030, 2020
<https://doi.org/10.5194/acp-20-2017-2020-supplement>
© Author(s) 2020. This work is distributed under
the Creative Commons Attribution 4.0 License.



Supplement of

The characteristics of atmospheric brown carbon in Xi'an, inland China: sources, size distributions and optical properties

Can Wu et al.

Correspondence to: Gehui Wang (ghwang@geo.ecnu.edu.cn)

The copyright of individual parts of the supplement might differ from the CC BY 4.0 License.

40 **Table List**

41 Table S1 Correlation coefficients between $\text{abs}_{\lambda=365\text{nm}}$ and organic carbon species during
42 sampling periods.

43

44 Table S2 Values of Q_{true} , Q_{robust} and average r for the modeling results during sampling
45 periods.

46

47

48

49 **Figure caption**

50 Table S1 Correlation coefficients (r) between $\text{abs}_{\lambda=365\text{ nm}}$ and organic carbon species during
51 sampling periods.

52

53 Fig. S2 Comparison of levoglucosan/mannosan and levoglucosan/galactosan ratios between
54 biomass fuel and the samples of this study. Hardwoods cited from Fine et al. (2004a,
55 2004b);Bari et al. (2010), softwood cited from Fine et al. (2004a, 2004b);Bari et al. (2010),
56 needles derived from Sullivan et al. (2014);Engling et al. (2006), leaves derived from Sullivan
57 et al. (2014);Schmidl et al. (2008), rice straw cited from Sheesley et al. (2003);Yan et al.
58 (2015), wheat straw derived from Yan et al. (2015).

59

60 Fig. S3 A comparison on the results measured by Anderson ($D_p < 2.1\mu\text{m}$) and the $\text{PM}_{2.5}$ filter
61 samples.

62

63 Fig. S4 Temporal variations of PAHs/OC and levoglucosan/OC during the haze period of
64 January 12th to 19th (corresponding to the cyan shadow in Figure 5) in Xi'an.

65

66 Fig. S5 Regression analysis for PAHs, OPAHs, nitrophenols, EC, and visibility. (a) PAHs,
67 OPAHs, nitrophenols, and EC vs. visibility, (b) PAHs/EC, OPAHs/EC, and nitrophenols/EC
68 vs. visibility.

69

70

71

72

73

74

75

76

77

78

79

80

81

82
83
84

Table S1 Correlation coefficients (r) between $abs_{\lambda=365nm}$ and organic carbon species during sampling periods.

	$abs_{\lambda=365nm}\text{-MeOH}$	
	Winter	Summer
Levogluconan	0.98	0.73
PAHs	0.95	0.73
OPAHs	0.97	0.86
Nitrophenols	0.89	0.78

85
86
87
88
89

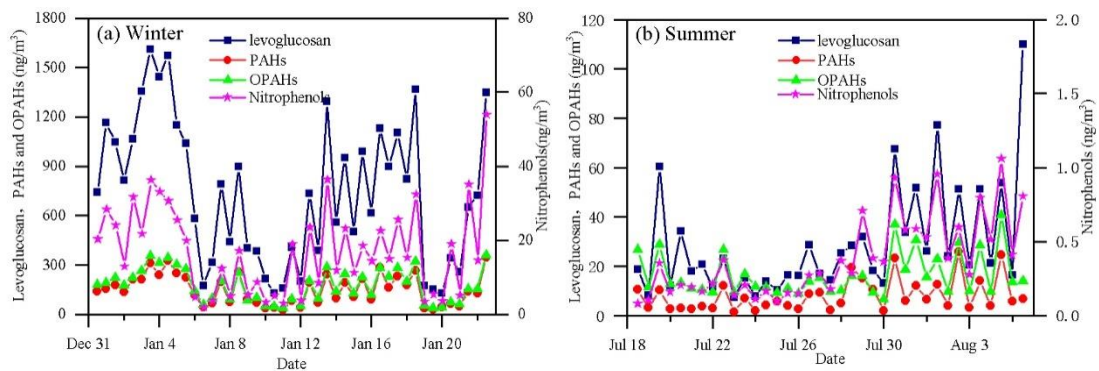
Note: all data are significant at the 0.01 level

90
91

Table S2 Values of Q_{true} , Q_{robust} and average r for the modeling results during sampling periods.

	Q_{true}	Q_{robust}	Average r
Sampling periods	724	718.7	0.98

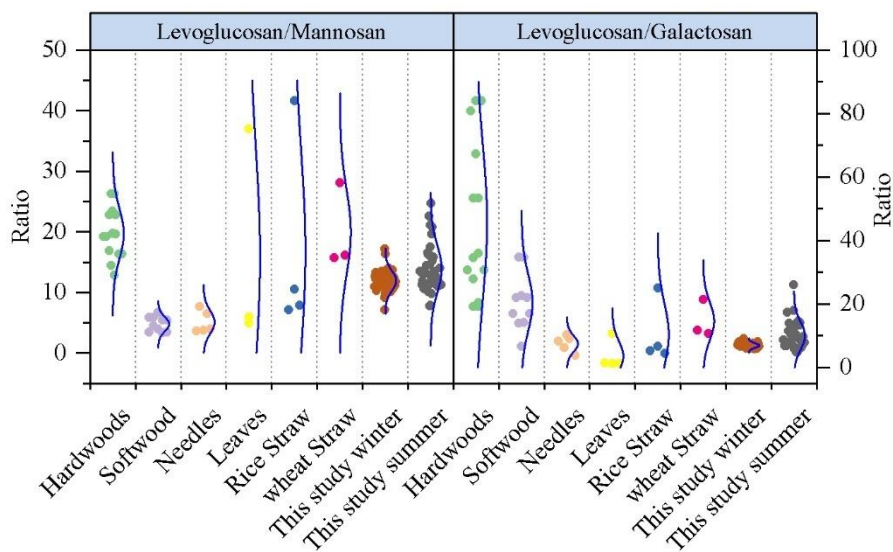
92
93
94
95
96



97
98
99

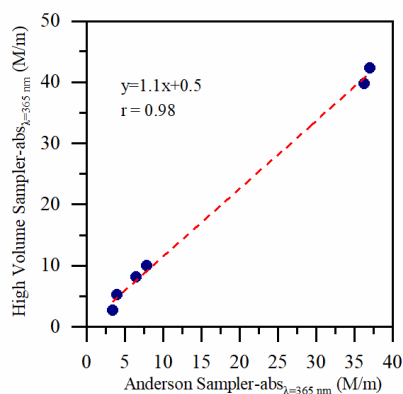
Fig. S1 Temporal variations of levoglucosan, PAHs, OPAHs, and nitrophenols during winter and summer.

100
101



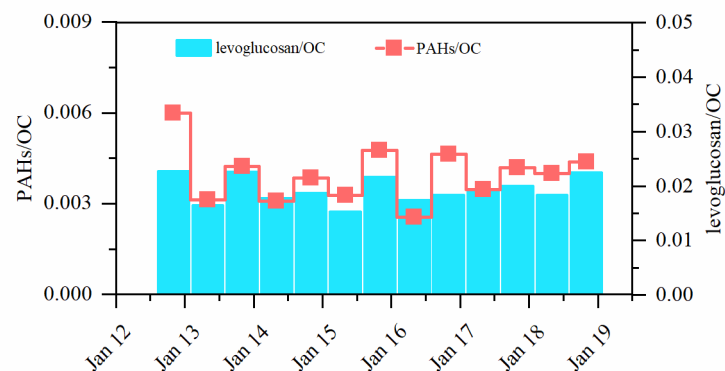
102
 103 Fig. S2 Comparison of levoglucosan/mannosan and levoglucosan/galactosan ratios between
 104 biomass fuels and the samples of this study. Hardwoods cited from Fine et al. (2004a,
 105 2004b);Bari et al. (2010), softwood cited from Fine et al. (2004a, 2004b);Bari et al. (2010),
 106 needles derived from Sullivan et al. (2014);Engling et al. (2006), leaves derived from Sullivan
 107 et al. (2014);Schmidl et al. (2008), rice straw cited from Sheesley et al. (2003);Yan et al.
 108 (2015), wheat straw derived from Yan et al. (2015).

109
 110



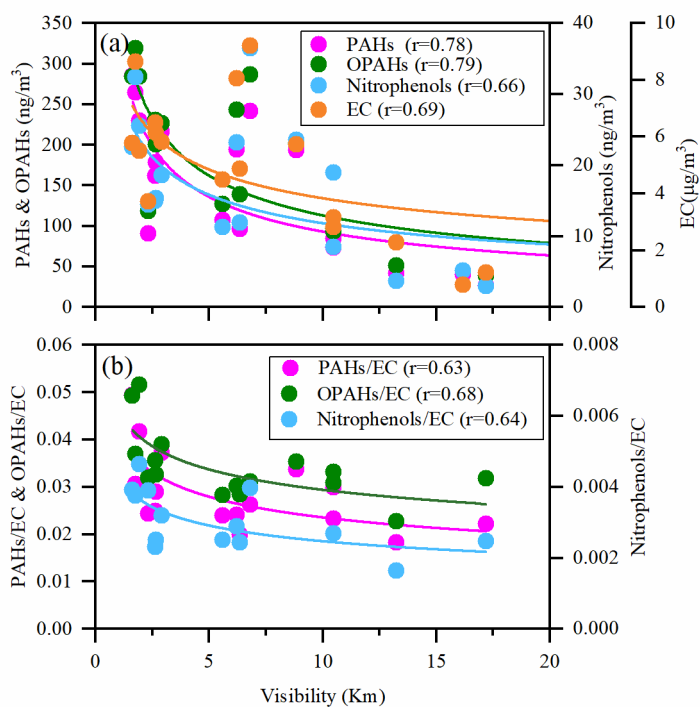
111
 112 Fig. S3 A comparison on the results measured by Anderson ($D_p < 2.1 \mu\text{m}$) and the $\text{PM}_{2.5}$ filter
 113 samples.

114
 115



116
117
118
119
120
121

Fig. S4 Temporal variations of PAHs/OC and levoglucosan/OC during the haze period of January 12th to 19th (corresponding to the cyan shadow in Figure 5) in Xi'an.



122

Fig. S5 Regression analysis for PAHs, OPAHs, nitrophenols, EC, and visibility. (a) PAHs, OPAHs, nitrophenols, and EC vs. visibility, (b) PAHs/EC, OPAHs/EC, and nitrophenols/EC vs. visibility.

126
127

References

129 Bari, M. A., Baumbach, G., Kuch, B., and Scheffknecht, G.: Temporal variation and impact of wood
130 smoke pollution on a residential area in southern Germany, Atmospheric Environment, 44,
131 3823-3832, 2010.
132 Engling, G., Carrico, C., Krelidenweis, S., Collett, J., Day, D. W., Lincoln, E., Hao, W., Iinuma, Y., and

133 Herrmann, H.: Determination of levoglucosan in biomass combustion aerosol by
134 high-performance anion-exchange chromatography with pulsed amperometric detection,
135 Atmospheric Environment, 40, 299-311, 2006.

136 Fine, P. M., Cass, G. R., and Simoneit, B. R. T.: Chemical characterization of fine particle emissions
137 from the fireplace combustion of wood types grown in the Midwestern and Western United States,
138 Environmental Engineering Science, 36, 387-409, 2004a.

139 Fine, P. M., Cass, G. R., and Simoneit, B. R. T.: Chemical characterization of fine particle emissions
140 from the wood stove combustion of prevalent United States tree species, Environmental
141 Engineering Science, 21, 705-721, 2004b.

142 Schmidl, C., Bauer, H., Dattler, A., Hitzenberger, R., Weissenboeck, G., Marr, I. L., and Puxbaum, H.:
143 Chemical characterisation of particle emissions from burning leaves, Atmospheric Environment,
144 42, 9070-9079, 2008.

145 Sheesley, R. J., Schauer, J. J., Chowdhury, Z., Cass, G. R., and Simoneit, B. R. T.: Characterization of
146 organic aerosols emitted from the combustion of biomass indigenous to South Asia, Journal of
147 Geophysical Research: Atmospheres, 108, n/a-n/a, 10.1029/2002jd002981, 2003.

148 Sullivan, A. P., May, A. A., Lee, T., McMeeking, G. R., Kreidenweis, S. M., Akagi, S. K., Yokelson, R.
149 J., Urbanski, S. P., and Collett Jr, J. L.: Airborne characterization of smoke marker ratios from
150 prescribed burning, Atmospheric Chemistry and Physics, 14, 10535-10545,
151 10.5194/acp-14-10535-2014, 2014.

152 Yan, C., Zheng, M., Sullivan, A. P., Bosch, C., Desyaterik, Y., Andersson, A., Li, X., Guo, X., Zhou, T.,
153 and Örjan, G.: Chemical characteristics and light-absorbing property of water-soluble organic
154 carbon in Beijing: Biomass burning contributions, Atmospheric Environment, 121, 4-12, 2015.

155